Journal of Ceramic Processing Research. Vol. 13, No. 3, pp. 278~282 (2012)

J O U R N A L O F
Ceramic Processing Research

Influence of the properties of corundum aggregates on the strength and slag resistance of refractory castables

Wen Yan*, Nan Li, Zheng Miao, Guangping Liu and Yuanyuan Li
The Key State Laboratory Breeding Base of Refractories and Ceramics, Wuhan University of Science and Technology, Wuhan, P.R. of China

Three refractory castables containing corundum aggregates with different porosities, average pore size and strength and the same matrices were fabricated. The effects of the properties of corundum aggregates on the strength and slag resistance of refractory castables were investigated through an X-ray diffractometer (XRD), scanning electron microscopy (SEM), mercury porosimetry measurements, etc. It was found that the properties of corundum aggregates have an important effect on the bulk density, porosity, compressive strength and slag resistance of refractory castables, but have little effect on the flexural strength of refractory castables. Compared with a castable containing white fused corundum aggregate (with a porosity of 4.2% and a bulk density of 3.62 g/cm^3), the castable containing a porous corundum aggregate (with a porosity of 42.0% and a bulk density of 2.29 g/cm^3) has a higher porosity of 35.7%, a lower bulk density of 2.44 g/cm^3, a lower but sufficient compressive strength (80.4 MPa) and a lower slag resistance, but has a similar flexural strength (20.3 MPa), and then has a potential application for a non-slag working lining of a ladle to decrease the consumption of energy and Al_2O_3 material.

Key words: Corundum aggregate, Properties, Refractory castables, Strength, Slag resistance.

Introduction

There is a large energy consumption in the iron and steel industry. Refractories, as the essential materials for furnaces and the parts used at high temperature, have a duty to save energy and resources. With an increased demand for saving high-quality resources and energy, more attention has been devoted to research on lightweight and heat-insulating refractories [1-7]. Traditionally lightweight refractories mainly consist of Al_2O_3-SiO_2 materials, which are acidic and have a low strength, can not be used as a working lining in a ladle [1-2]. Neutral and basic lightweight refractories with a high strength and high slag resistance are required [2].

Al_2O_3-MgO refractory castables have been widely used as working linings in ladles due to their excellent properties and easy installation [2, 3, 5-12]. In order to fabricate lightweight Al_2O_3-MgO refractory castables, the bulk density of a dense aggregate must be decreased. A decrease of the bulk density of an aggregate may affect the strength and slag resistance of a castable, which determines whether a lightweight castable could be used as a working lining of a ladle.

The effects of porosity and the pore size distribution on the strength of aggregates have been investigated [3-4]. It is found that a smaller pore size and a homogenous pore distribution are helpful to improve the strength of aggregates, and porous periclase-spinel, spinel and corundum-spinel ceramics with a small pore size and high strength were obtained through optimizing pore structures [3]. If the porous aggregates have enough strength, the castables would have enough strength, which have the potential application as working linings of furnaces.

In addition, the corrosion of the castables containing porous periclase-spinel, spinel and corundum-spinel aggregates has been investigated. It is found that castables containing porous aggregates with different phase compositions have different slag resistances, and when the porous aggregate is the same, the slag resistance could be enhanced through changing the composition of the matrix [6, 7]. If the porous aggregates have a high slag resistance similar to the matrices, refractory castables would have enough slag resistance to be used as working lining of ladles, including the slag working lining [6].

But until now, when the matrices have the same composition and a similar microstructure, after changing the porosity and strength of the corundum aggregate of refractory castables, how the strength and slag resistance of refractory castables would evolve has still not been understood. In order to study the possibility to use refractory castables containing lightweight corundum aggregate as the working lining of a ladle, the effects of the properties of corundum aggregate on the strength and slag resistance of refractory castables were investigated, and some results were addressed.

*Corresponding author:
Tel: +86-027-68862511
Fax: +86-027-68862121
E-mail: yanwenref@yahoo.com.cn

Table 1. Bulk densities, apparent porosities and strengths of corundum aggregates.

	Apparent porosity (%)	Bulk density (g/cm^3)	Numerical tube pressure (%)
A	4.2	3.62	92.4
B	24.4	2.95	65.8
C	42.0	2.29	48.1

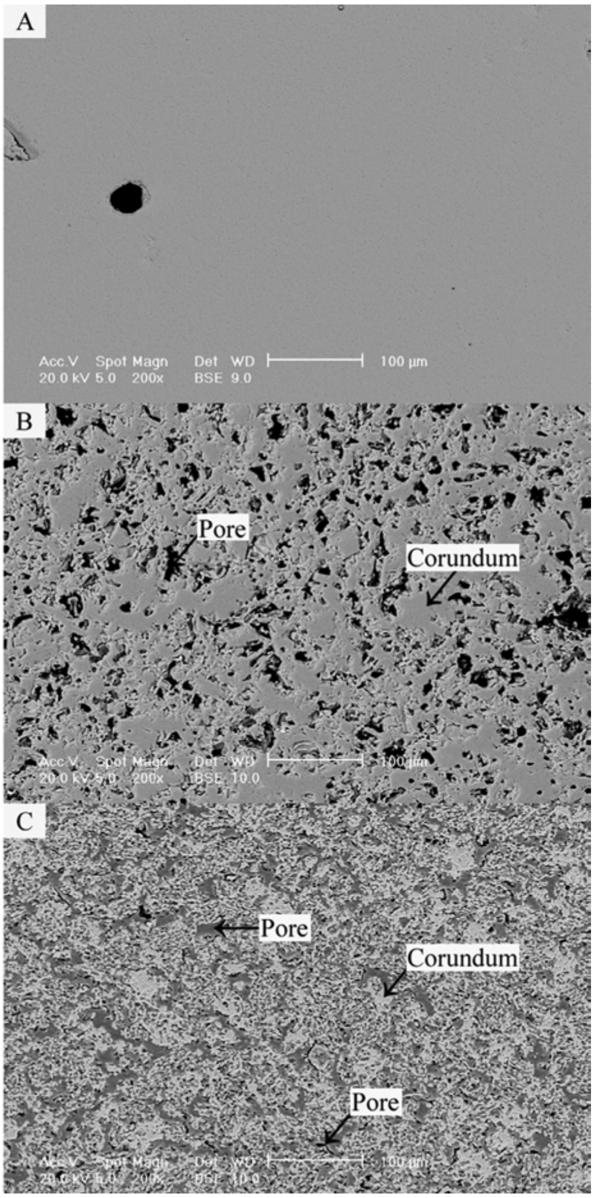

Fig. 1. Microstructures of aggregates A, B and C.

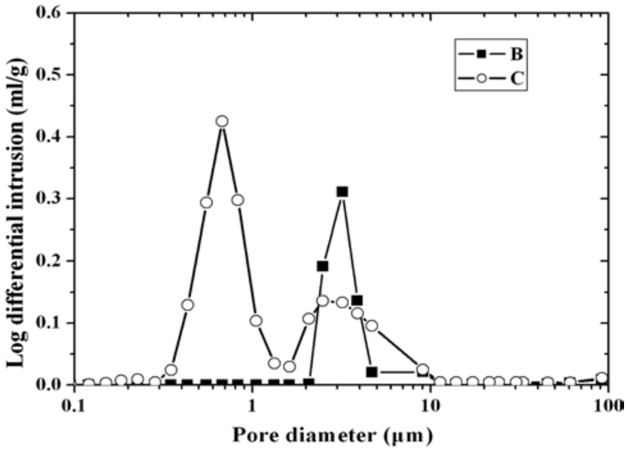

Fig. 2. Pore size distributions of aggregates B and C.

Experimental

Three refractory castables were prepared with the same matrix but different aggregates. The apparent porosities, bulk densities, and numerical tube pressure of three corundum aggregates are listed in Table 1. The strength of corundum aggregates were evaluated by the numerical tube pressure. The numerical tube pressure was conducted as follows: Pack aggregates with diameter of 5-4 mm in a Φ50 mm mould to a height of 50 mm, weighing the mass of aggregates as m0, and then press it with a pressure of 50 MPa for 10 seconds; then sift the pressed aggregates by a sieve with a diameter of 3 mm; eventually, weigh the mass of the aggregates with a diameter bigger than 3 mm as m1; consequently the numerical tube pressure was given by $m1/m0 \times 100\%$.

The microstructures and pore size distributions of the aggregates are shown in Fig. 1 and Fig. 2, respectively. The aggregate A is densified white fused corundum. But the aggregates B and C contain many pores, and their average pore sizes are 3.25 μm and 0.94 μm, respectively. Three refractory castables were named as castable A, castable B and castable C according to their different aggregates. The chemical composition of the slag is listed in Table 2. The particle size distribution of aggregates, aggregate content (65 vol%) and matrix content (35 vol%) were kept unchanged for all batches of castables. Water contents of castable A, B and C were 5.5 wt%, 8.5 wt% and 11.4 wt%, respectively. Rectangular parallelepiped specimens with a size of 140 mm length×25 mm width×25 mm thickness were cast for the porosity, density and strength measurements. Cubic blocks with 30 mm diameter and 40 mm deep

Table 2. Chemical composition of slag (wt%).

Al_2O_3	MgO	SiO_2	CaO	MnO	Fe_2O_3
2.45	7.95	14.48	45.78	2.46	26.47

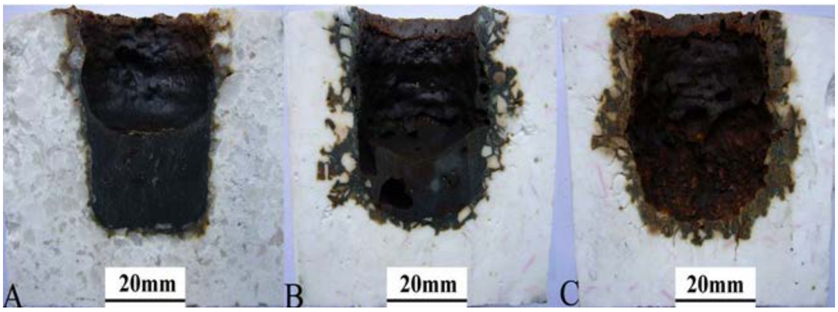

Fig. 3. Crucibles after slag testing (vertical cut).

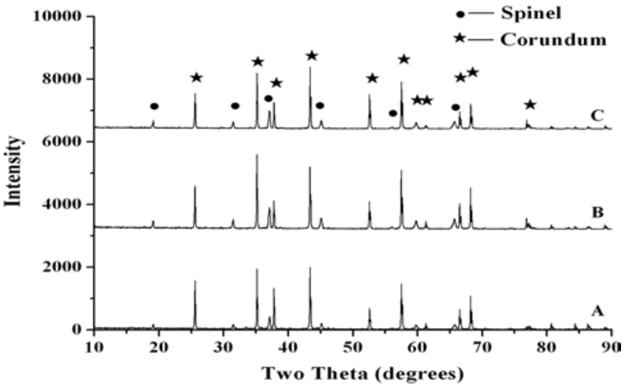

Fig. 4. X-ray diffraction patterns of castables sintered at 1600 ºC.

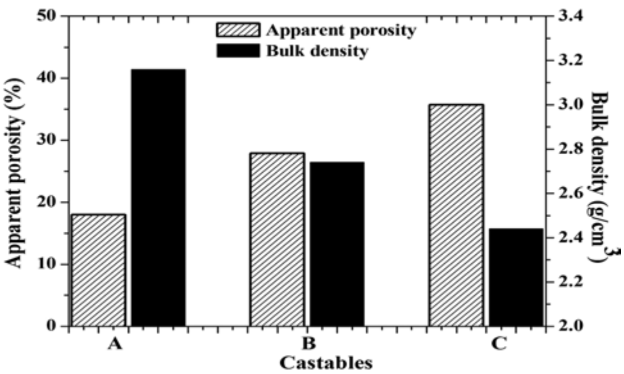

Fig. 5. Apparent porosities and bulk densities of castables sintered at 1600 ºC.

holes were vibrocast for the crucible corrosion tests. They were cured for 24 h at room temperature before drying at 110 °C for a further 24 h. The dried rectangular parallelepiped specimens and cubic blocks filled with 30 g slag were heated at 1600 °C for 3 h in an electric chamber furnace and then furnace-cooled to room temperature.

After corrosion testing, crucibles were cross-sectioned perpendicular to the slag-refractory interface, as shown in Fig. 3. The actual corroded and penetrated areas in each sample were measured by counting pixels. Corrosion here is defined as regions of refractory completely replaced by slag. The corrosion index Ic and penetration index Ip are obtained by the following equation: $I_{C(P)}=S_{C(P)}/S_O*100\%$; S_O is the original section area of the crucible inner chamber; S_C, the section area of the refractory completely replaced by the slag; S_P, the penetrated section area.

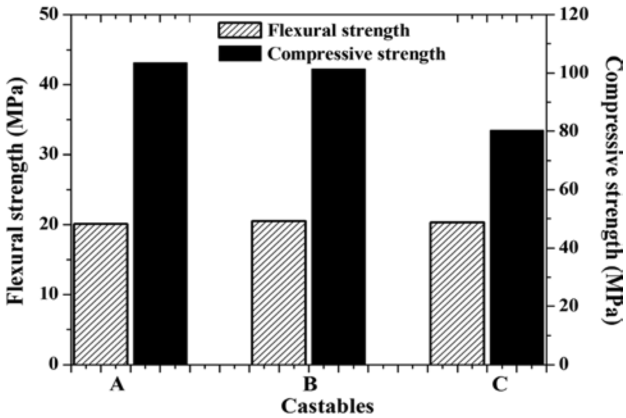

Fig. 6. Flexural and compressive strengths of castables sintered at 1600 ºC.

Phase analysis was carried out by an X-ray diffractometer (Philips Xpert TMP) with a scanning speed of 2° per minute. Apparent porosities and bulk densities of castables were measured by Archimedes' principle with water as the medium. Flexural and compressive strengths of sintered samples at room temperature were measured. The pore size distributions and average pore sizes were measured by mercury porosimetry measurements (AutoPore IV 9500, Micromeritics Instrument Corporation). The microstructure and glass phase composition were measured by a scanning electron microscope with EDAX (Philips XL30).

Results and discussion

Phase identification

XRD patterns of castables sintered at 1600 ºC are shown in Figure 4. It is found that the phases in castables A, B and C are corundum (Al_2O_3) and spinel ($MgO \cdot Al_2O_3$).

Bulk density, apparent porosity and strength

Apparent porosities and bulk densities of castables sintered at 1600 ºC are given in Fig. 5. With an increase in the porosity of aggregates, the apparent porosities of castables increase, and the bulk densities decrease. The apparent porosity and bulk density of

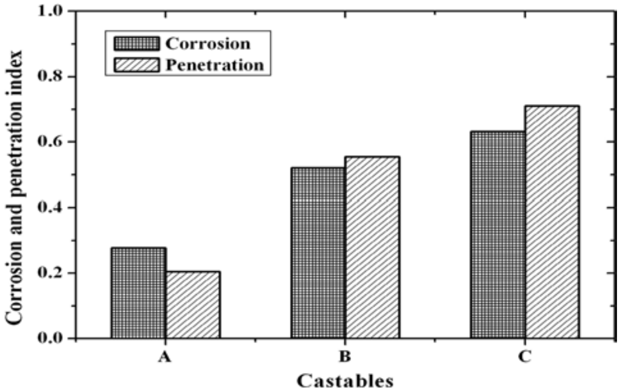

Fig. 7. Corrosion and penetration indexes of castables.

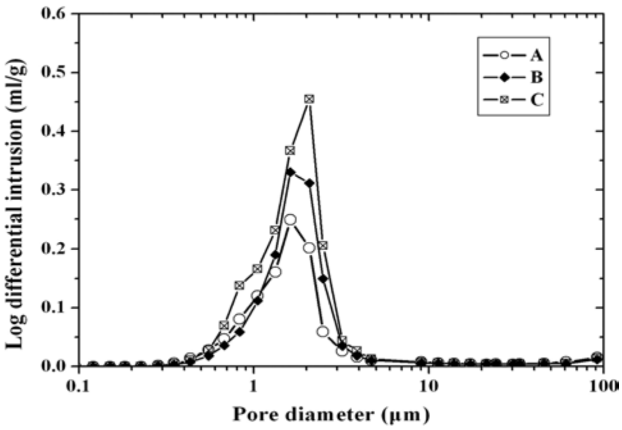

Fig. 8. Pore size distributions of matrices A, B and C.

castable A are 18.0% and 3.16 g/cm^3 respectively, but the apparent porosity and bulk density of castable C are 35.7% and 2.44 g/cm^3 respectively.

The flexural strength and compressive strength of castables sintered at 1600 ºC are shown in Figure 6. For the three castables containing aggregates with different porosities, the strength of the aggregates decreases with increasing porosity, the flexural strengths are almost the same, about 20 MPa (Table 1 and Fig. 6). When the porosity of the aggregate was increased from 4.2% to 24.4%, the compressive strength decreases slightly from 103.5 MPa to 101.3 MPa, but with a further increase of porosity to 42.0%, the compressive strength decreases to 80.4 MPa.

This means that when the porosity of corundum aggregates increases from 4.2% to 42.0%, the bulk density of castable decreases obviously, compressive strength decreases slightly, but the flexural strength changes little.

Corrosion results

The slag corrosion and penetration indexes are shown in Figure 7. It can be seen, with an increase in the porosity of aggregates, the corrosion and penetration indexes increase obviously. This means that the slag resistances of castables decrease with an increase in the porosity of corundum aggregates.

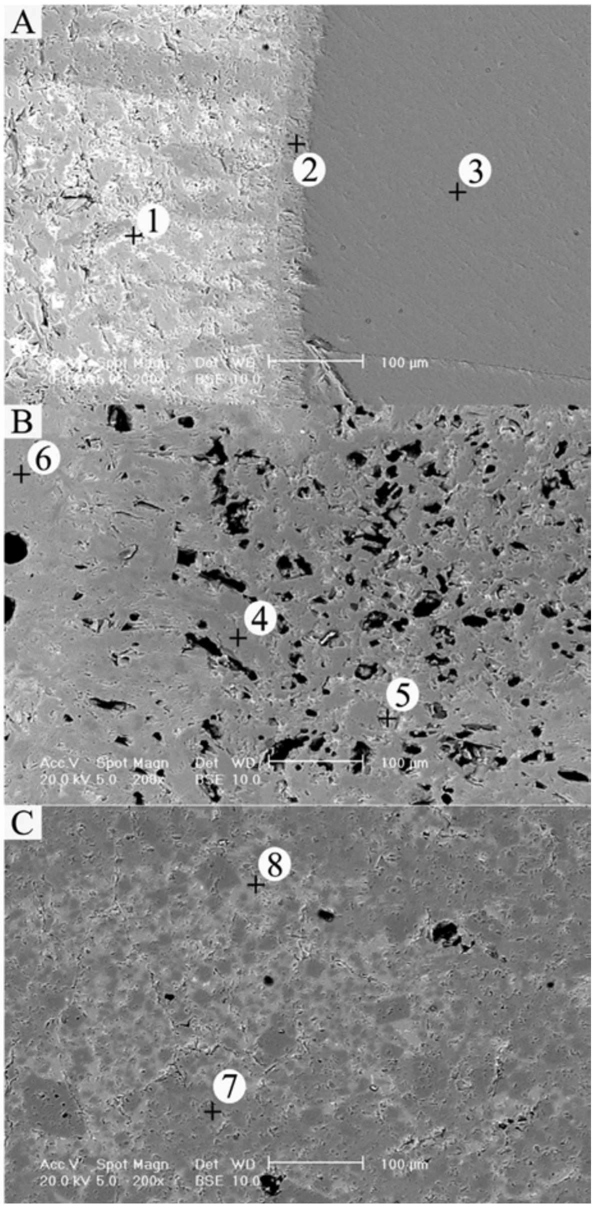

Fig. 9. Typical BSE images of aggregates in three castables.

Discussion

In order to investigate the influence of aggregate' properties on the performance of refractory castable, the pore size distributions of matrices A, B and C are given in Fig. 8. It is found that the pore size distributions of matrices A, B and C are similar, but the peak value of matrix C is the highest and the peak value of matrix A is the lowest, which means the porosity of matrix C is the highest and the porosity of matrix A is the lowest, which may come from the different water content in the castables. In addition, the average pore size of matrices A, B and C are 1.95 µm, 2.01 µm and 2.03 µm, respectively, almost the same. It is concluded that the similar flexural strengths of the three castables may depend on the similar matrices, because the matrices have a similar pore size distribution and the

Table 3. Typical results of EDS analysis at Fig. 9 (wt%)

	1	2	3	4	5	6	7	8
Al_2O_3	15.08	89.87	100	100	08.86	50.22	100	
SiO_2	13.69				04.57			12.51
CaO	60.37	10.13			86.57	37.67		69.33
Fe_2O_3	10.86					12.11		18.16

same average pore size of the matrices; while the decreasing compressive strength may come from the different aggregates, because an increase in the porosity of aggregates decreases the strength, as listed in Table 1.

Typical back scattered electron (BSE) images of aggregates in the three castables and the corresponding typical results of EDS analysis are given in Fig. 9 and Table 3, respectively. In castable A, a CA6 ($CaO\cdot 6Al_2O_3$) layer (about 20 μm thickens) is formed between the slag and aggregate, resulting in the dissolution of refractory into the slag is indirect, and then the slag resistance is enhanced. But in castable C, the aggregate totally penetrated by the slag. The poor penetration resistance of porous aggregate C results in the lowest slag resistance. If the thickness of wall between pores in porous aggregate C is more than 40 μm, CA6 layers would possibly be formed between the slag and aggregates, and then the slag resistance of castable would be enhanced.

Considering the strength and slag resistance, the castables containing the porous corundum aggregate C have a high strength and the lowest bulk density, and thus have a potential application to be used as a non-slag working lining of a ladle to decrease the consumption of energy and Al_2O_3 material.

Conclusions

The porosity and strength of a corundum aggregate have a strong effect on the bulk density, porosity, compressive strength and slag resistance of castables, but have little effect on the flexural strength. The detailed results are as follows:

(1) Increasing the porosity of aggregates from 4.2% to 42.0%, the bulk density and compressive strength of castable decrease, but the flexural strength changes little. When the porosity of porous aggregate is 42.0%, the castable has a high porosity of 35.7%, a low bulk density of 2.44 g/cm^3, a high flexural strength (20.3 MPa) and a high compressive strength (80.4 MPa).

(2) Increasing the porosity of a corundum aggregate, the slag penetration resistance of a castable deteriorates, resulting in the slag resistance becoming worse.

Acknowledgments

The authors would like to thank the 973 Program Earlier Research Project (No. 2012CB722702), and the Puyang Refractories Co., Ltd for financially supporting this work.

References

1. M.N. Dunaeva, Refract. Ind. Ceram. 47 (2006) 199-200.
2. W. Yan, N. Li, B. Han, X. Fang, and G. Liu, Ceram-Silikáty 54 (2010) 315-319.
3. W. Yan, N. Li, and B. Han, Am. Ceram. Soc. Bull. 84 (2005) 9201-9203.
4. W. Yan, N. Li, and B.Q. Han, J. Ceram. Process. Res. 11 (2010) 388-391.
5. W. Yan, N. Li, and B. Han, Sci. Sinter. 41(2009) 275-281.
6. W. Yan, N. Li, and B. Han, Int. J. Appl. Ceram. Technol. 5 (2008) 633-640.
7. W. Yan, N. Li, and B. Han, Interceram: Refractories Manual (2009) 25-28.
8. R. Chen, P. He, N. Wang, J. Mou, and F. Gan, in Proceedings of UNITECR, Oct 2003, edited by T. Yamato, p. 670.
9. L.A. Díaz, T. Torrecillas, A.H. de Aza, and P. Pena, J. Eur. Ceram. Soc. 27(2007) 4623-4631.
10. H. Sarpoolaky, S. Zhang, B.B. Argent, and W.E. Lee, J. Am. Ceram. Soc. 84 (2001) 426-434.
11. Y. Ko, J. Am. Ceram. Soc. 83 (2000) 2333-2335.
12. P. Korgul, D.R. Wilson, and W.E. Lee, J. Eur. Ceram. Soc. 17 (1997) 77-84.